quantum reports

MDPI

Article

Non-Relativistic Energy Spectra of the Modified Hylleraas Potential and Its Thermodynamic Properties in Arbitrary Dimensions

Collins Okon Edet [1,2,*], Jonathan E. Osang [2], Norshamsuri Ali [1,*], Emmanuel Paul Agbo [2], Syed Alwee Aljunid [1], Rosdisham Endut [1], Emmanuel B. Ettah [2], Reza Khordad [3], Akpan Ndem Ikot [4] and Muhammad Asjad [1]

[1] Faculty of Electronic Engineering Technology, Universiti Malaysia Perlis, Kangar 01000, Perlis, Malaysia; syedalwee@unimap.edu.my (S.A.A.); rosdisham@unimap.edu.my (R.E.); asjad_qau@yahoo.com (M.A.)
[2] Department of Physics, Cross River University of Technology, Calabar PMB 1123, Nigeria; jonathanosang@yahoo.com (J.E.O.); emmanuelpaulagbo@gmail.com (E.P.A.); emmanuelettah@gmail.com (E.B.E.)
[3] Department of Physics, College of Sciences, Yasouj University, Yasouj 75918, Iran; rezakh2025@yahoo.com
[4] Theoretical Physics Group, Department of Physics, University of Port Harcourt, East/West Road, Choba PMB 5323, Nigeria; akpan.ikot@uniport.edu.ng
* Correspondence: collinsokonedet@crutech.edu.ng (C.O.E.); norshamsuri@unimap.edu.my (N.A.)

Abstract: In this study, the solutions of the Schrodinger equation (SE) with modified Hylleraas potential in arbitrary dimensions was obtained using the asymptotic iteration method (AIM) to obtain the energy and wave functions, respectively. The energy equation was used to obtain the thermal properties of this system. The effect of the potential parameters and dimensions on the energy spectra and thermal properties was scrutinized thoroughly. It was found that the aforementioned affects the thermal properties and energy spectra, respectively. In addition, we also computed the numerical energy spectra of the MHP for the first time and discussed it in detail. The results of our study can be applied to molecular physics, chemical physics, etc.

Keywords: asymptotic iteration method (AIM); Schrodinger equation; Hylleraas potential

Citation: Edet, C.O.; Osang, J.E.; Ali, N.; Agbo, E.P.; Aljunid, S.A.; Endut, R.; Ettah, E.B.; Khordad, R.; Ikot, A.N.; Asjad, M. Non-Relativistic Energy Spectra of the Modified Hylleraas Potential and Its Thermodynamic Properties in Arbitrary Dimensions. *Quantum Rep.* **2022**, *4*, 238–250. https://doi.org/10.3390/quantum4030016

Academic Editor: Gerald B. Cleaver

Received: 10 March 2022
Accepted: 8 July 2022
Published: 29 July 2022

1. Introduction

Quantum mechanics (QM) is a tool required for the proper understanding of how a particle behaves in a micro-physical domain [1–3]. QM gives a logical mathematical framework that brings about a good understanding of areas of physics which includes plasmas, superconductor and semiconductor devices, physics of solids, etc. [4]. In addition, QM encompasses all disciplines that are contained in modern physics such as thermodynamics, statistical physics, particle physics, optics, etc. Even beyond the areas of physics, QM is very important in the investigation of the basic dynamics of biological and chemical trends [5].

Erwin Schrodinger formulated the concept of wave mechanics in 1926 and thus proved to be one of the major breakthroughs in the area, as his QM formulation was widely accepted. His formulation has proven to be more insightful by being able to properly explain the dynamics of microscopic matter with what is popularly known as the Schrödinger equation (SE): a second-order differential equation [4].

The energy spectrum and wave function of a system is obtained when the SE equation is being solved with a particular interaction potential [6]. The interactions of particles within a system determine the form of the potential in use. The different forms of potentials include harmonic, Coulomb, Kratzer potential [7], Cornell [8], perturbed Yukawa [9] and pseudoharmonic [10], Morse potential [11], Deng–Fan–Eckart potential, etc.; some

combinations of these potentials have been done as well as extensive research to solve the SE (approximately and exactly) [12–15].

Reviewing a range of research work on the analytical solutions of the SE shows that multiple forms of interaction potentials have been used to reveal the fundamental dynamics of a variety of systems with varying degrees of success [16]. In the study of a host of physical systems, confining potentials play a very important role. Its importance spans across various areas of physics including atomic and molecular physics, solid state physics, nuclear physics, particle physics, chemical physics, etc. [8,14].

Relating to this, the adoption of the SE for the solution of some potentials of interest for which $l \neq 0$ is difficult or could be said to be quasi-impossible. Some potentials including the Coulomb [17], Harmonic potential [18], Kratzer potential [7], etc., have an exception to this, are they are easily solved by the SE equation. The s-wave ($l = 0$) case can only be solved exactly [7]; in contrast, the cases where we have $l \neq 0$, we implement numerous approximation schemes that eventually approximate the centrifugal term in the SE. This process will lead to the approximation of the bound state solutions [19,20].

For quantum mechanical studies, an important thing to note is that the exact solutions of the SE play a very significant role; one notable importance is that these quantum mechanical studies offer a scope that is interesting to investigate regarding applications in diverse areas of physics. As earlier buttressed, the SE is exactly solvable only for limited interaction potentials including the Harmonic and Coulomb potentials. It remains an enormous task to apply this for complex potentials such as the exponential-type potentials; this has continued to remain an issue for diverse researchers and offers a good challenge for the expansion of techniques that already exist and also for the proper exploration of new methods to the end that the catalogue of exactly solvable problems can be enlarged [21–24].

On this note, there is a need to properly study the modified Hylleraas potential (MHP) mainly because it has not been properly studied in the past. The aim of this kind of study will be the enhancing of this MHP by solving with the SE and also the evaluation of its thermodynamic properties.

To dive into history, mathematical and theoretical physicists have developed a wide range of mathematical methods for aid in the solution of the SE; these methods ranged from numerical to analytical techniques. The interesting fact is that irrespective of the techniques that were being used for the solution (except for some algebraic configurations), the solutions obtained are similar. Some of these techniques include the factorization method [4,25], shape invariant supersymmetry quantum mechanics (SUSYQM) approach [26], asymptotic iteration method (AIM) [27–30], Nikiforov–Uvarov (NU) method [23,31,32], Parametric NU method [33], formula method [34], Wentzel, Krammers, Brullion and Jeffery (WKBJ) method [35,36], exact quantization rule (EQR) [37,38], and proper quantization rule (PQR) [20]. These techniques are utilized in both non-relativistic and relativistic equations for diverse potentials.

In the present work, we consider a general form of a confining potential, which is the MHP; this is with the goal of increasing the catalogue of analytically solvable potentials and their possible adoption in studying physical systems.

Thermodynamics is a very important part of physics that has its applications in diverse areas. In extension, it offers an analysis of macroscopic thermodynamic quantities at the molecular level. It also goes further to investigate the thermodynamic activities of systems which comprise a large number of particles by adopting the probability theory. One of the most vital advances of physics in the early twentieth century has been the exposition of the macroscopic theory of thermodynamics in terms of the more abstract microscopic statistical mechanics [39–41].

Various researchers have carried out studies on the thermodynamic properties for a quantum system. Okorie et al. [42] assessed the thermodynamic properties for the modified Kratzer plus screened Coulomb potential. Ikot et al. [43] assessed the thermodynamic functions of exponential-type molecular potential in D dimensions. Ikot et al. [44] acquired the thermal properties of the improved screened Kratzer potential (ISKP) model.

2. The Hylleraas Potential (HP) and the Modified Hylleraas Potential (MHP)

The solutions of wave equations in relativistic and non-relativistic QM have recently received great attention. A variety of researchers have made progress in evaluating their energy and that of the corresponding wave functions. Nevertheless, this is due to its applications in studying several physical systems of interest. HP is one of those potentials that cannot be solved exactly as earlier buttressed. The potential was proposed as an intermolecular potential and is one of the best potential models considered to explain the vibrational energy of diatomic molecules [45].

Ikot et al. [46] noted that the HP is a special case of the multiparameter exponential-type potential. Since Hylleraas presented this potential, not much work has been reported on the bound state solution, whether in a relativistic and non-relativistic regime. Again, Ikot [23] presented a modified version of the Hylleraas potential, which is given by

$$V(r) = \frac{V_0}{b}\frac{a - e^{-2\alpha r}}{1 - e^{-2\alpha r}}. \tag{1}$$

where α is the screening parameter. Ever since then, several adjustments have been proposed, but the focus of this study will be on Equation (1). It is worthy to point out here that since Hylleraas initiated this potential, very minute research has used it.

3. Solutions of the Schrodinger Equation with Modified Hylleraas Potential

The motion of a particle in a spherically symmetric potential in D dimensions is written as [32,43,47]

$$\frac{d^2R_{nl}(r)}{dr^2} + \frac{2\mu}{\hbar^2}\left[E_{nl} - V(r) - \frac{\hbar^2(D+2l-1)(D+2l-3)}{8\mu r^2}\right]R_{nl}(r) = 0. \tag{2}$$

Due to the fact that the above equation cannot be solved analytically for $l \neq 0$ due to the centrifugal term, the Greene and Aldrich approximation scheme [19] to the centrifugal term is used; this is given as

$$\frac{1}{r^2} = \frac{4\alpha^2 e^{-2\alpha r}}{(1 - e^{-2\alpha r})^2}. \tag{3}$$

It is convenient to point out here that for a short-range potential, the relation Equation (3) is a good approximation to $1/r^2$, implying that it is not a good approximation to the centrifugal barrier when the screening parameter α becomes large. Thus, the approximation is valid when $\alpha r << 1$ [19]. By subsituting Equation (1) in Equation (2) and using the Greene and Aldrich Approximation in Equation (3), one obtains

$$\frac{d^2R_{nl}(\varrho)}{d^2\varrho} + \frac{1}{\varrho}\frac{dR_{nl}(\varrho)}{d\varrho} - \frac{(\varepsilon_{nl} + \varsigma)\varrho^2 + (2\varepsilon_{nl} + \varsigma + \bar{\varsigma} - \gamma)\varrho - (\varepsilon_{nl} + \bar{\varsigma})}{\varrho^2(1-\varrho)^2}R_{nl}(\varrho) = 0, \tag{4}$$

where we have used the following dimensionless notations $\varepsilon_{nl} = -\frac{\mu E_{nl}}{2\hbar^2\alpha^2}$, $\varsigma = \frac{\mu V_0}{2\hbar^2 b\alpha^2}$, $\bar{\varsigma} = \varsigma a$ and $\gamma = (D+2l-1)(D+2l-3)/4$. In the above equation, we have used $\varrho = e^{-2\alpha r}$. In order to solve Equation (4) using AIM [27], we propose the following physical radial wavefunction $R_{nl}(\varrho) = \varrho^{\nu}(1-\varrho)^{\delta}f_{nl}(\varrho)$ where $\nu = \sqrt{\varepsilon_{nl} + \bar{\varsigma}}$ and $\delta = 1/2 + \sqrt{\gamma + 1/4}$. Now, by substituting the ansats in Equation (4), we obtain

$$\frac{d^2f_{nl}(\varrho)}{d^2\varrho} - \lambda_0(\varrho)\frac{df_{nl}(\varrho)}{d\varrho} - s_0(\varrho)f_{nl}(\varrho) = 0, \tag{5}$$

where

$$\lambda_0(\varrho) = \frac{(2\nu + 2\delta + 1)\varrho - (2\nu + 1)}{\varrho(1-\varrho)} \text{ and } s_0(\varrho) = \frac{(\nu+\delta)^2 - (\varepsilon_{nl} + \varsigma)}{\varrho(1-\varrho)}.$$

With the aid of the quantization condition as discussed in Ref. [27], we arrive at the following eigenvalues expressions

$$\begin{aligned}
\theta_0 &= \begin{vmatrix} \lambda_0(\varrho) & s_0(\varrho) \\ \lambda_1(\varrho) & s_1(\varrho) \end{vmatrix} = 0 \Leftrightarrow \nu_0 = -\delta \pm \sqrt{\varepsilon_{nl} + \varsigma}, \\
\theta_1 &= \begin{vmatrix} \lambda_1(\varrho) & s_1(\varrho) \\ \lambda_2(\varrho) & s_2(\varrho) \end{vmatrix} = 0 \Leftrightarrow \nu_1 = -1 - \delta \pm \sqrt{\varepsilon_{nl} + \varsigma}, \\
&: = \begin{vmatrix} : & : \\ : & : \end{vmatrix} = 0 \Leftrightarrow :=:, \\
\theta_n &= \begin{vmatrix} \lambda_n(\varrho) & s_n(\varrho) \\ \lambda_{n+1}(\varrho) & s_{n+1}(\varrho) \end{vmatrix} = 0 \Leftrightarrow \nu_n = -n - \delta \pm \sqrt{\varepsilon_{nl} + \varsigma},
\end{aligned} \tag{6}$$

and then the explicit forms of ε_{nl} and E_{nl}, respectively, are given by

$$\varepsilon_{nl} = -\bar{\varsigma} + \frac{[\varsigma - \bar{\varsigma} - (n + \sqrt{\gamma + 1/4} + 1/2)^2]^2}{4(n + \sqrt{\gamma + 1/4} + 1/2)^2}$$

and

$$E_{nl} = a\frac{V_0}{b} - \frac{\hbar^2\alpha^2}{2\mu}\left(\frac{\varsigma(1-a) - (n + \sqrt{\gamma + /1/4} + 1/2)^2}{n + \sqrt{\gamma + /1/4} + 1/2}\right)^2. \tag{7}$$

Figure 1 shows the variation of energy E_{nl} values of the MHP against various potential parameters. In Figure 1a, we plot E_{nl} as a function of V_0/b for different values of $D = 1$ (red curve), 2 (green curve), 3 (black curve), 4 (blue curve) and 5 (purple curve). We notice that the value of E_{nl} decreases as the ration V_0/b increases. The value of E_{nl} increases as function of the parameter a at a fixed value of the ration $V_0/b = 0.2$, where the color scheme is the same as in Figure 1a, as shown in Figure 1b. In Figure 1c, we show that the value of E_{nl} increases as the screening parameter α increases.

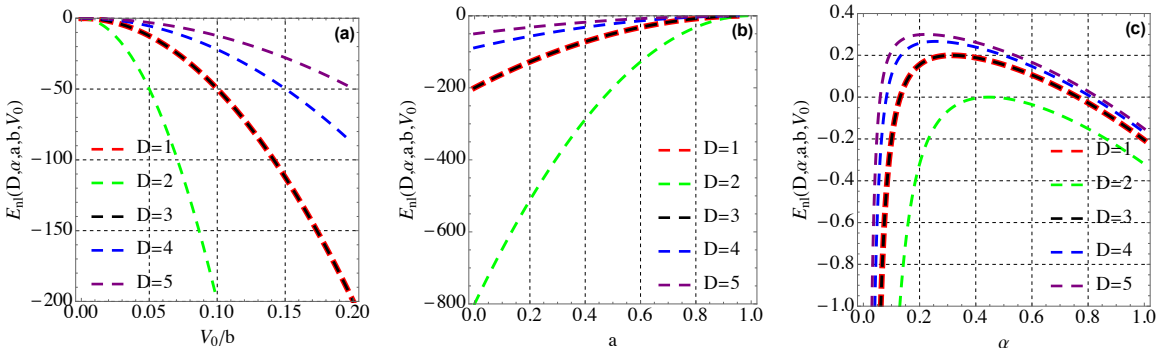

Figure 1. Variation of E_{nl} energy values of the MHP versus (**a**) ratio V_0/b (**b**) parameter a (**c**) screening parameter α for different values of D, $D = 1$ (red curve), 2 (green curve), 3 (black curve), 4 (blue curve) and 5 (purple curve).

In this study, the bound state solution of the modified Hylleraas potential has been found in an arbitrary D-dimension via the asymptotic iteration method (AIM). From Equation (7) and Table 1, it is clear that the two inter-dimensional states are degenerate whenever $(n, l, D) \rightarrow (n, l \pm 1, D \mp 2) \Rightarrow E^D_{nl} = E^{D\mp2}_{n,l\pm1}$. Thus, a knowledge of $E^D_{n,l}$ for $D = 2$ to 5 provides the information necessary to find $E^D_{n,l}$ for other higher dimensions. It is also observed that the energy increases as the screening parameter increases.

Table 1. Numerical non-relativistic energy spectra of the MHP.

State	α	$D=1$	$D=2$	$D=3$	$D=4$	$D=5$
1s	0.025	−7.7003100	−31.8003000	−7.7003100	−3.2225300	−1.6503100
	0.050	−1.7012500	−7.8012500	−1.7012500	−0.5568060	−0.1512500
	0.075	−0.5917010	−3.3583700	−0.5917010	−0.0645409	0.1249650
	0.100	−0.2050000	−1.8050000	−0.2050000	0.1061110	0.2200000
2s	0.025	−1.6503100	−3.2225300	−1.6503100	−0.9203130	−0.5225350
	0.050	−0.1512500	−0.5568060	−0.1512500	0.0387500	0.1431940
	0.075	0.1249650	−0.0645409	0.1249650	0.2149650	0.2650890
	0.100	0.2200000	0.1061110	0.2200000	0.2750000	0.3061110
2p	0.025	−7.7003100	−3.2225300	−1.6503100	−0.9203130	−0.5225350
	0.050	−1.7012500	−0.5568060	−0.1512500	0.0387500	0.1431940
	0.075	−0.5917010	−0.0645409	0.1249650	0.2149650	0.2650890
	0.100	−0.2050000	0.1061110	0.2200000	0.2750000	0.3061110
3s	0.025	−0.5225350	−0.9203130	−0.5225350	−0.2819450	−0.1253130
	0.050	0.1431940	0.0387500	0.1431940	0.2069130	0.2487500
	0.075	0.2650890	0.2149650	0.2650890	0.2960540	0.3166320
	0.100	0.3061110	0.2750000	0.3061110	0.3256120	0.3387500
3p	0.025	−1.6503100	−0.9203130	−0.5225350	−0.2819450	−0.1253130
	0.050	−0.1512500	0.0387500	0.1431940	0.2069130	0.2487500
	0.075	0.1249650	0.2149650	0.2650890	0.2960540	0.3166320
	0.100	0.2200000	0.2750000	0.3061110	0.3256120	0.3387500
3d	0.025	−1.6503100	−0.9203130	−0.5225350	−0.2819450	−0.1253130
	0.050	−0.1512500	0.0387500	0.1431940	0.2069130	0.2487500
	0.075	0.1249650	0.2149650	0.2650890	0.2960540	0.3166320
	0.100	0.2200000	0.2750000	0.3061110	0.3256120	0.3387500
4s	0.025	−0.1253130	−0.2819450	−0.1253130	−0.0175965	0.0596875
	0.050	0.2487500	0.2069130	0.2487500	0.2777620	0.2987500
	0.075	0.3166320	0.2960540	0.3166320	0.3310700	0.3416320
	0.100	0.3387500	0.3256120	0.3387500	0.3480860	0.3550000
4p	0.025	−0.5225350	−0.2819450	−0.1253130	−0.0175965	0.0596875
	0.050	0.1431940	0.2069130	0.2487500	0.2777620	0.2987500
	0.075	0.2650890	0.2960540	0.3166320	0.3310700	0.3416320
	0.100	0.3061110	0.3256120	0.3387500	0.3480860	0.3550000
4d	0.025	−0.5225350	−0.2819450	−0.1253130	−0.0175965	0.0596875
	0.050	0.1431940	0.2069130	0.2487500	0.2777620	0.2987500
	0.075	0.2650890	0.2960540	0.3166320	0.3310700	0.3416320
	0.100	0.3061110	0.3256120	0.3387500	0.3480860	0.3550000
4f	0.025	−0.5225350	−0.2819450	−0.1253130	−0.0175965	0.0596875
	0.050	0.1431940	0.2069130	0.2487500	0.2777620	0.2987500
	0.075	0.2650890	0.2960540	0.3166320	0.3310700	0.3416320
	0.100	0.3061110	0.3256120	0.3387500	0.3480860	0.3550000

For completeness sake, the wave function of the system is given as

$$R_{nl}(\varrho) = (-1)^n \mathcal{N}_{nl} \frac{\Gamma(2\nu+n+1)}{\Gamma(2\nu+1)} \varrho^{\nu}(1-\varrho)^{\delta}\, {}_2F_1(-n, 2(\nu+\delta)+n; 2\nu+1; \varrho) \tag{8}$$

where $\mathcal{N}_{nl}$ is the normalization constant and ${}_2F_1(-n, 2(\nu+\delta)+n; 2\nu+1; \varrho)$ is the hypergeometric function.

4. Thermal and Magnetic Properties of Modified Hylleraas Potential (MHP)

In this section, we study the thermal properties of the modified Hylleraas potential. Using a direct summation over all possible vibrational energy levels that are assessable to the system, we can compute the vibrational partition function. Given the energy spectrum in Equation (7), the partition function $Z(\beta)$ of the MHP at finite temperature T is obtained with the Boltzmann–Gibbs statistics as [14,29,48–50].

$$Z(\beta) = \sum_{n=0}^{n_{max}} e^{-\beta E_n} \tag{9}$$

where $\beta = 1/k_B T$, k_B is the Boltzmann constant and $n = 0, 1, 2, 3, \ldots, n_{max}$ is the vibrational quantum number with n_{max} as the upper bound of the viberational quantum number, and it is obtained by setting $\frac{dE_n}{d_n} = 0$ and is given by

$$n_{max} = -\left(\frac{1}{2} + \sqrt{\gamma + 1/4}\right) \pm \sqrt{\varsigma(1-a)}. \tag{10}$$

The summation in Equation (9) can be replaced by an integral. Therefore, Equation (9) can be written as

$$Z(\beta) = \int_{\tilde{\sigma}}^{n_{max}+\tilde{\sigma}} e^{-\beta\left(\frac{\eta_0}{\rho^2}+\eta_1\rho^2+\eta_2\right)} d\rho, \tag{11}$$

where $\rho = n + \tilde{\sigma}$ and the integral is evaluated in the region $\tilde{\sigma} < \rho < n_{max} + \tilde{\sigma}$, and the following notations have been introduced for mathematical simplicity: $\eta_0 = \hbar^2\alpha^2Q^2/(2\mu)$, $\eta_1 = \eta_0/Q^2$ and $\eta_2 = -(P + 2Q)\eta_1$. On evaluating the integral in Equation (11), we obtain the partition function of the modified Hylleraas potential as follows

$$Z(\beta) = \frac{e^{\beta}\sinh(\beta\sqrt{\eta_0\eta_1})}{2\sqrt{-\beta\eta_1}}\left\{\mathrm{Erf}[\sqrt{-\beta}(\sqrt{\eta_0} - t_1^2\sqrt{\eta_1})/t_1] - \mathrm{Erf}[\sqrt{-\beta}(\sqrt{\eta_0} + t_2^2\sqrt{\eta_1})/t_2]\right\}, \tag{12}$$

where $t_1 = \tilde{\sigma}$ and $t_2 = n_{max} + \tilde{\sigma}$. This expression represents the classical partition function. The reason is that Equation (12) does not contain quantum corrections.

In Figure 2, we show plots of the partition function $Z(\beta)$ as a function of V_0/b (a), a (b), parameter D (c), and screening parameter α for different values of the $\beta = 0.01\,\mathrm{K}^{-1}$ (red curve), $0.02\,\mathrm{K}^{-1}$ (green curve), $0.05\ \mathrm{K}^{-1}$ (black curve). Figure 2a clearly shows that the partition function decreases with increasing V_0/b. Figure 2b displays the partition function as a function of a for different values of β. It is seen that the partition function first decreases and then increases with increasing a. Figure 2c displays the partition function as a function of dimensional parameter D for different values of β. It is seen that the partition function decreases with increasing dimension D and then increases with rising D. Figure 2d shows the plot of partition function as a function of screening parameter α with different values of β. We notice that in the region $0 < \alpha < 0.01$, the partition function first decreases and then rises as the screening parameter α rises.

In what follows, all thermodynamic properties of the MHP, such as the free energy, mean energy, the entropy and specific heat, can be obtained from the partition function $Z(\beta)$. These thermodynamic functions for the MHP will be scrutinized in the following sections.

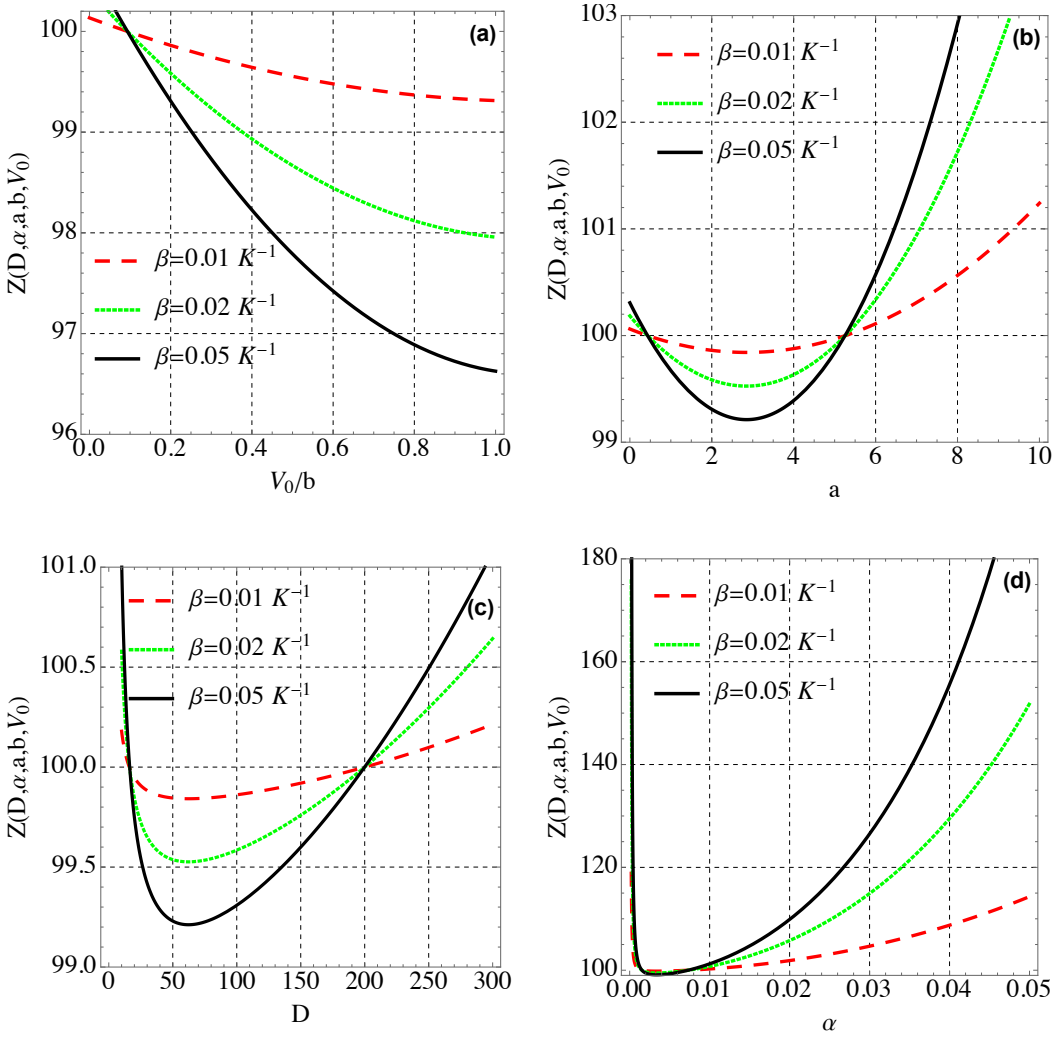

Figure 2. Partition function $Z(\beta)$ as a function of; (**a**) V_0/b, (**b**) parameter a, (**c**) D and (**d**) screening parameter α for different values of $\beta = 0.01\,\mathrm{K}^{-1}$ (red curve), $0.02\,\mathrm{K}^{-1}$ (green curve), $\beta = 0.05\,\mathrm{K}^{-1}$ (black curve).

4.1. Free Energy

In this subsection, the free energy $F(\beta, D, a, b, V_0) = -\frac{1}{\beta}\ln(Z(\beta))$ for MHP is studied. Figure 3 shows plots of the free energy $F(\beta, D, a, b, V_0)$ versus V_0/b, (b) parameter a, (c) dimensions D and (d) screening parameter α for different values of $\beta = 2.0\,\mathrm{K}^{-1}$ (red curve), $4.0\,\mathrm{K}^{-1}$ (green curve), 6.0 K^{-1} (black curve). Figure 3a clearly shows that the free energy first increases and then decreases with increasing V_0/b for different values of β. We show the plot of the free energy as a function of a different values of β. The free energy decreases with increasing a. Figure 3c displays the free energy as a function of dimension, D for different values of β. It is seen that the free energy increases monotonically with increasing D. Figure 3d shows the plot of free energy as a function of screening parameter α with different values of β. In this figure, we see that the free energy first rises with the rising screening parameter and then decreases, as shown in Figure 3d.

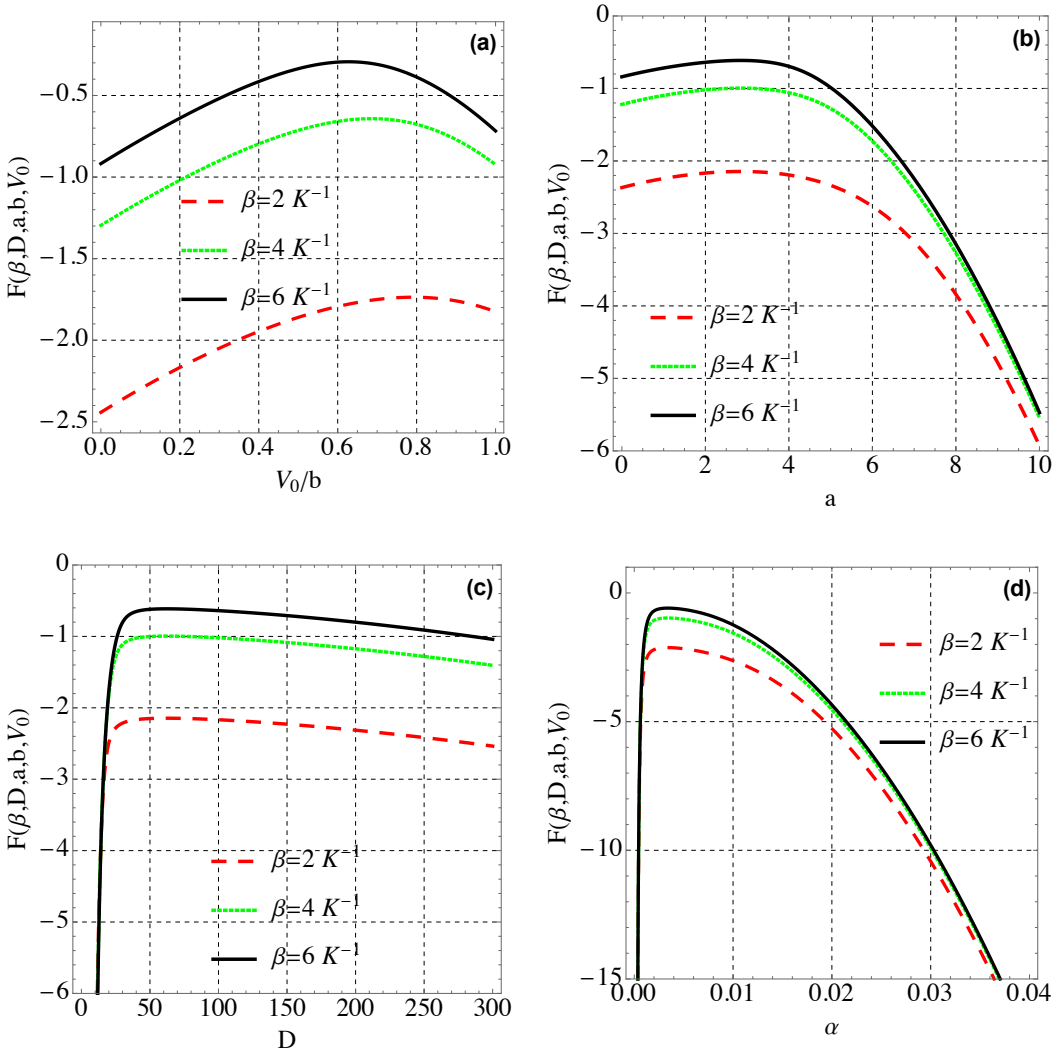

Figure 3. (**a**) Plots of free energy $F(\beta, D, a, b, V_0)$ versus V_0/b, (**b**) parameter a, (**c**) D and (**d**) screening parameter α for different values of $\beta = 2.0\,\mathrm{K}^{-1}$ (red curve), $4.0\,\mathrm{K}^{-1}$ (green curve), $6.0\,\mathrm{K}^{-1}$ (black curve).

4.2. Mean Energy

In this subsection, the mean energy $U(\beta, D, a, b, V_0) = -\dfrac{d\ln Z(\beta)}{d\beta}$ of the MHP is analyzed. In Figure 4, we show plots of the mean energy $U(\beta, D, a, b, V_0)$ as a function of β, dimensions-D and other potential parameters. Figure 4a clearly shows that the mean energy increases and then decreases with V_0/b for different values of $\beta = 1.0\,\mathrm{K}^{-1}$ (red curve), $2.0\,\mathrm{K}^{-1}$ (green curve), and $3.0\ \mathrm{K}^{-1}$ (black curve). Figure 4b shows the plot of the mean energy as a function of a different values of β. The mean energy decreases with increasing a. Figure 4c displays the mean energy as a function of D for different values of β. It is seen that the mean energy first increases and then decreases with increasing D. Figure 4d shows the plot of mean energy as a function of α with different values of β. In this figure, we see that in the region $0 < \alpha < 0.005$, the mean energy first rises with rising screening parameters and then decreases.

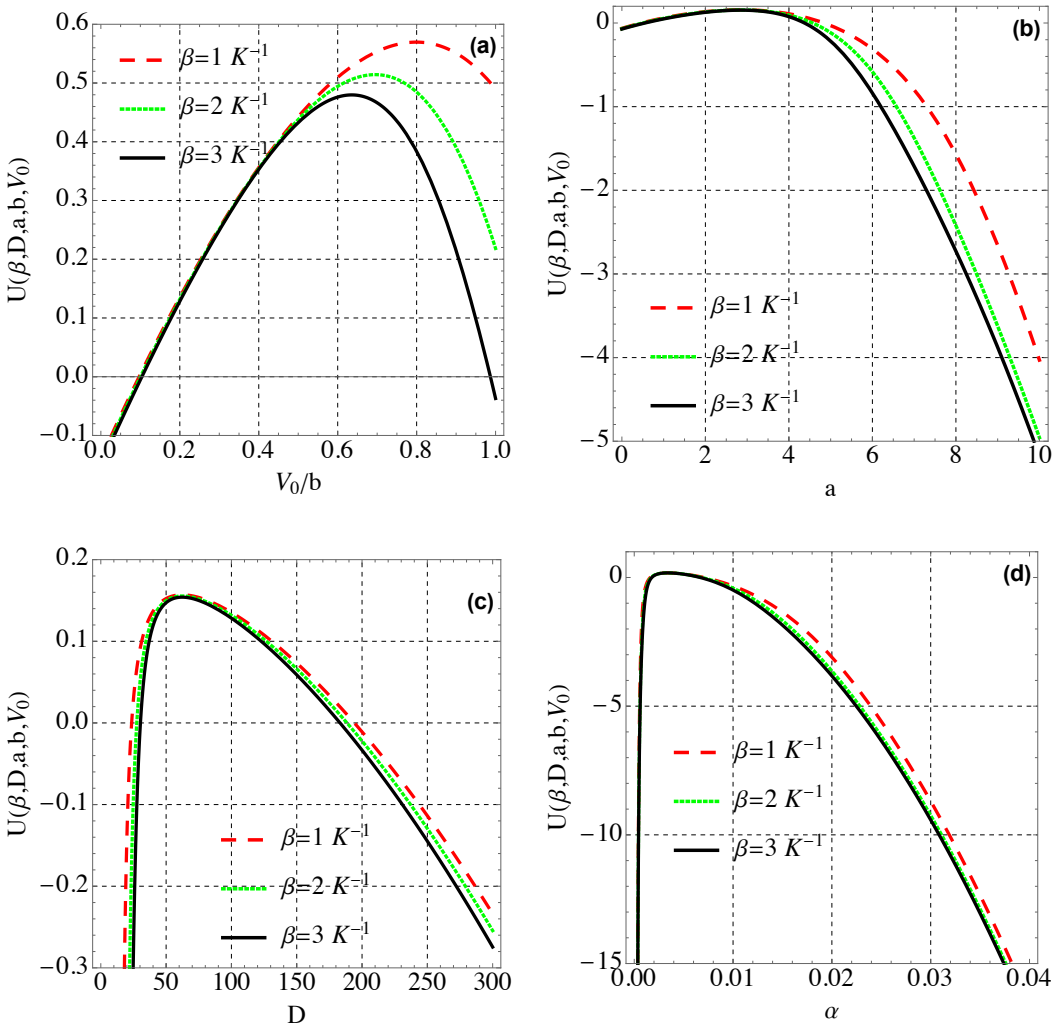

Figure 4. (**a**) Mean energy $U(\beta, D, a, b, V_0)$ as a function of V_0/b, (**b**) parameter a, (**c**) D and (**d**) screening parameter α for $\beta = 1.0\,\mathrm{K}^{-1}$ (red curve), $2.0\,\mathrm{K}^{-1}$ (green curve), and $3.0\,\mathrm{K}^{-1}$ (black curve).

4.3. Spacific Heat Capacity

An analysis of the specific heat capacity $C(\beta, D, a, b, V_0) = \beta^2 \frac{d^2 \ln Z(\beta)}{d\beta^2}$ of the system is extensively carried out in Figure 5. Figure 5 shows plots of the specific heat capacity as a function of β, dimensions D, and other potential parameters. Figure 5a shows that the plot of the specific heat capacity as a function of V_0/b for $\beta = 0.01\,\mathrm{K}^{-1}$ (red curve), $0.02\,\mathrm{K}^{-1}$ (green curve), and $0.05\,\mathrm{K}^{-1}$ (black curve). The specific heat capacity decreases with increasing the ration V_0/b. Figure 5b shows the plot of the specific heat capacity as a function of a with different values of β. The specific heat capacity decreases with increasing the value of a. Figure 5c displays the specific heat capacity as a function of dimension D for different values of β. It is seen that the specific heat capacity increases with increasing D. Figure 5d shows the plot of specific heat capacity as a function of screening parameter α with different values of β. It noticed that the specific heat capacity increases and then decreases as the screening parameter increases.

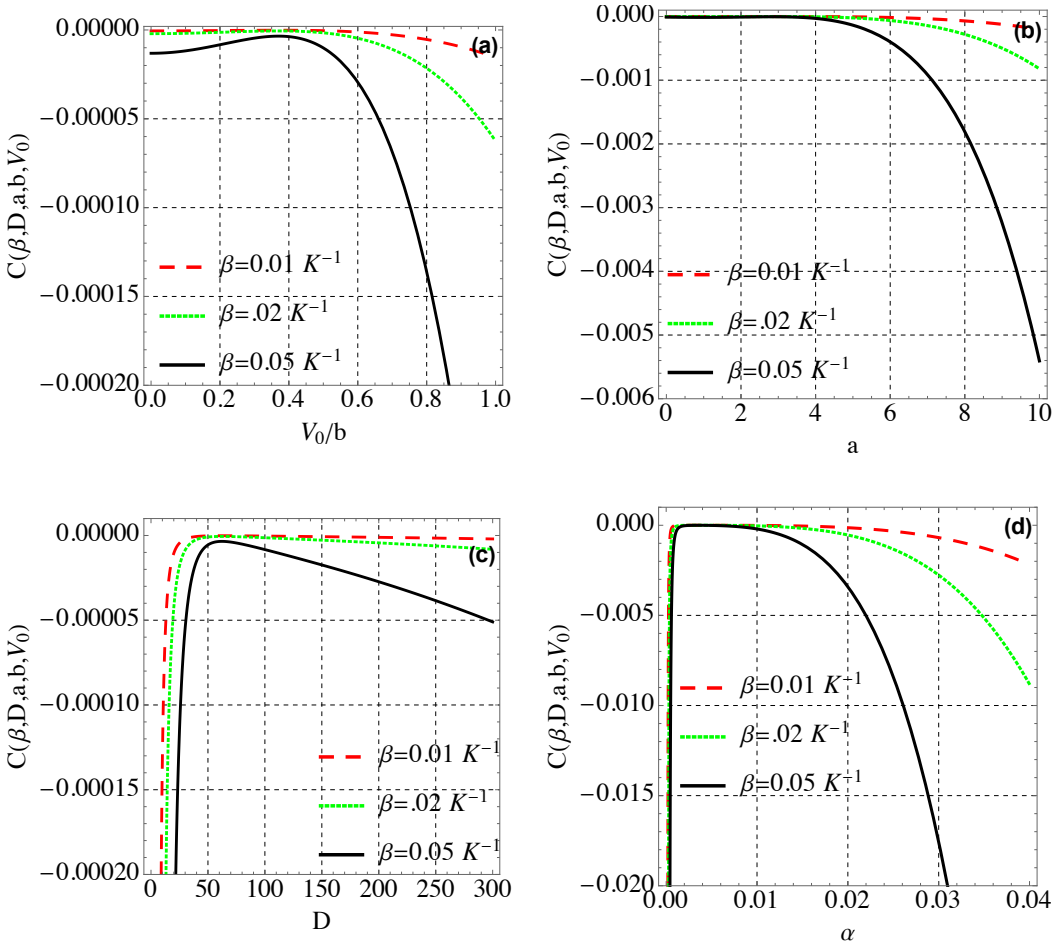

Figure 5. (**a**) Plots of specific heat capacity $C(\beta, D, a, b, V_0)$ as a function of V_0/b, (**b**) parameter a, (**c**) dimension D, and (**d**) screening parameter α for $\beta = 0.01\,\mathrm{K}^{-1}$ (red curve), $0.02\,\mathrm{K}^{-1}$ (green curve), and $0.05\,\mathrm{K}^{-1}$ (black curve).

4.4. Entropy

Here, the entropy $S(\beta, D, a, b, V_0) = \ln Z(\beta) - \beta \frac{d \ln Z(\beta)}{d\beta}$ of MHP is studied. Figure 6 shows plots of the entropy $S(\beta, D, a, b, V_0)$ as a function of V_0/b, (b) parameter a, (c) D and (d) screening parameter α for $\beta = 0.01\,\mathrm{K}^{-1}$ (red curve), $0.02\,\mathrm{K}^{-1}$ (green curve), and $0.05\,\mathrm{K}^{-1}$ (black curve). Figure 6a clearly shows that the entropy decreases with increasing V_0/b and decreases with increasing parameter a, as shown in Figure 6b. Figure 6c displays the entropy as a function of D for different values of β. It is seen that the entropy increases first and then decreases with increasing dimension D. Figure 6d shows the plot of entropy as a function of α with different values of β. We see that the entropy increases first and then decreases with rising screening parameter α.

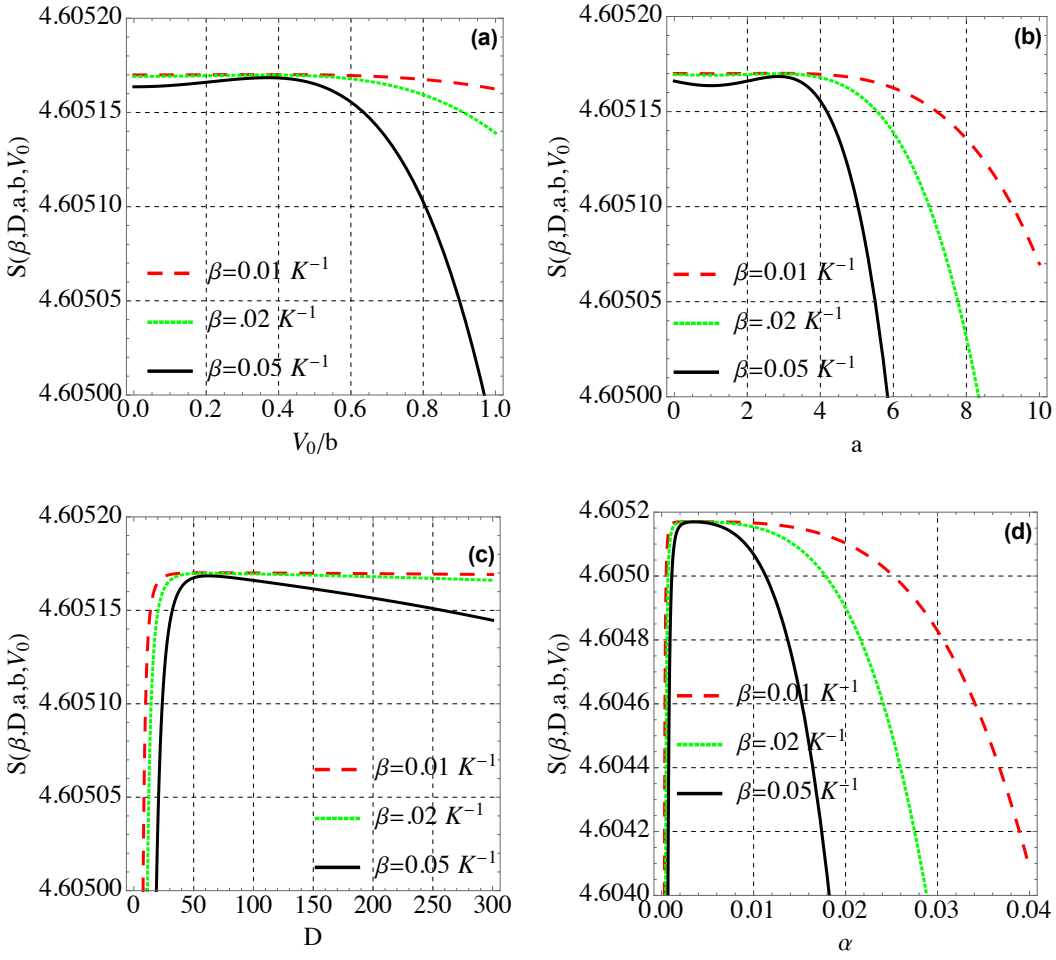

Figure 6. (**a**) Entropy $S(\beta, D, a, b, V_0)$ versus V_0/b, (**b**) parameter a, (**c**) D and (**d**) screening parameter α for $\beta = 0.01\,\mathrm{K}^{-1}$ (red curve), $0.02\,\mathrm{K}^{-1}$ (green curve), $0.05\,\mathrm{K}^{-1}$ (black curve).

5. Conclusions

In this paper, we obtained the bound state solutions of the Schrodinger equation with the modified Hylleraas potential in arbitrary dimensions using the asymptotic iteration method (AIM). The energy and wave functions were obtained, respectively. With the energy obtained, we evaluated the partition function, which was used to analyze the thermodynamic properties of the model. From our graphical analysis, we show that the thermal properties and energy spectra of the MHP depend on the potential parameters.

Author Contributions: Conceptualization, C.O.E., E.P.A. and S.A.A.; methodology, R.E.; software, E.B.E., E.P.A. and J.E.O.; validation, C.O.E. and S.A.A.; formal analysis, R.K.; in-vestigation, R.K.; resources, R.K.; data curation, C.O.E.; writing—original draft preparation, A.N.I., J.E.O., N.A. and M.A.; writing—review and editing. All authors have read and agreed to the published version of the manuscript.

Funding: The research has been carried out under Fundamental Research Grant Scheme project FRGS/1/2020/STG07/UNIMAP/02/03 provided by Ministry of Higher Education of Malaysia (MOHE)

Data Availability Statement: The datasets used and/or analyzed during the current study are available from the corresponding author on reasonable request.

Conflicts of Interest: The authors declare no conflict of interest.

References

1. Schrodinger, E. Quantisation as a problem of characteristic values. *Ann. Phys.* **1926**, *79*, 361.
2. Schrodinger, E. An undulatory theory of the mechanics of atoms and molecules. *Phys. Rev.* **1926**, *28*, 1049.
3. Schrodinger, E. Quantisierung als eigenwertproblem. *Ann. Phys.* **1926**, *385*, 437. [CrossRef]
4. Dong, S.H. *Factorization Method in Quantum Mechanics*; Springer Science & Business Media: Berlin/Heidelberg, Germany, 2007; Volume 150.
5. Sakurai, J.J. *Modern Quantum Mechanics*, revised ed.; Addison Wesley: Boston, MA, USA, 1993.
6. Antia, A.D.; Essien, I.E.; Umoren, E.B.; Eze, C.C. Solutions of relativistic Klein–Gordon equation with equal scalar and vector shifted Hulthen plus angle dependent potential. *Adv. Phys. Theor. Appl.* **2015**, *47*, 45.
7. Berkdemir, C. Application of the Nikiforov-Uvarov method in quantum mechanics. In *Theoretical Concepts of Quantum Mechanics*; IntechOpen: London, UK, 2012.
8. Abu-Shady, M.; Edet, C.O.; Ikot, A.N. Non-relativistic quark model under external magnetic and Aharanov–Bohm (AB) fields in the presence of temperature-dependent confined Cornell potential. *Can. J. Phys.* **2021**, *99*, 1024. [CrossRef]
9. Rajabi, A.A.; Hamzavi, M. Approximate analytical solutions of the perturbed Yukawa Potential with Centrifugal Barrier. *Z. Naturforschung A* **2013**, *68*, 454. [CrossRef]
10. Oyewumi, K.J.; Akinpelu, F.O. Exactly Complete Solutions Pseudoharmonic Potential N-Dimensions. *Int. J. Theor. Phys.* **2008**, *47*, 1039. [CrossRef]
11. Girifalco, L.A.; Weizer, V.G. Application of the Morse potential function to cubic metals. *Phys. Rev.* **1959**, *114*, 687. [CrossRef]
12. Edet, C.O.; Amadi, P.O.; Onyeaju, M.C.; Okorie, U.S.; Sever, R.; Rampho, G.J.; Abdullah, H.Y.; Salih, I.H.; Ikot, A.N. Thermal properties and magnetic susceptibility of Hellmann potential in Aharonov–Bohm (AB) flux and magnetic fields at zero and finite temperatures. *J. Low Temp. Phys.* **2021**, *202*, 83. [CrossRef]
13. Edet, C.O.; Okorie, K.O.; Louis, H.; Nzeata-Ibe, N.A. Any l-state solutions of the Schrodinger equation interacting with Hellmann–Kratzer potential model. *Indian J. Phys.* **2019**, *94*, 243. [CrossRef]
14. Edet, C.O.; Okorie, U.S.; Osobonye, G.; Ikot, A.N.; Rampho, G.J.; Sever, R. Thermal properties of Deng–Fan–Eckart potential model using Poisson summation approach. *J. Math. Chem.* **2020**, *58*, 989. [CrossRef]
15. Okoi, P.O.; Edet, C.O.; Magu, T.O. Relativistic Treatment of the Hellmann-generalized Morse potential. *Rev. Mex. Física* **2020**, *66*, 1. [CrossRef]
16. Antia, A.D.; Ikot, A.N.; Hassanabadi, H.; Maghsoodi, E. Bound state solutions of Klein–Gordon equation with Mobius square plus Yukawa potentials. *Indian J. Phys.* **2013**, *87*, 1133. [CrossRef]
17. Edet, C.O.; Okorie, U.S.; Ngiangia, A.T.; Ikot, A.N. Bound state solutions of the Schrodinger equation for the modified Kratzer potential plus screened Coulomb potential. *Indian J. Phys.* **2020**, *94*, 425. [CrossRef]
18. Ikhdair, S.M.; Sever, R. Relativistic two-dimensional harmonic oscillator plus cornell potentials in external magnetic and AB fields. *Adv. High Energy Phys.* **2013**, *2013*, 562959. [CrossRef]
19. Greene, R.L.; Aldrich, C. Variational wave functions for a screened Coulomb potential. *Phys. Rev. A* **1976**, *14*, 2363. [CrossRef]
20. Serrano, F.A.; Gu, X.Y.; Dong, S.H. Qiang–Dong proper quantization rule and its applications to exactly solvable quantum systems. *J. Math. Phys.* **2010**, *51*, 082103. [CrossRef]
21. Falaye, B.J. Any ℓ-state solutions of the Eckart potential via asymptotic iteration method. *Cent. Eur. J. Phys.* **2012**, *10*, 960. [CrossRef]
22. Oyewumi, K.J.; Titiloye, E.O.; Alabi, A.B.; Falaye, B.J. Bound states of pseudo-harmonic oscillator in the presence of magnetic field. *J. Niger. Math. Soc.* **2016**, *35*, 460.
23. Ikot, A.N. Solution of Dirac equation with generalized hylleraas potential. *Commun. Theor. Phys.* **2013**, *59*, 268. [CrossRef]
24. Ikot, A.N.; Okorie, U.S.; Rampho, G.J.; Abdullah, H.Y. Approximate energy spectra and statistical mechanical functions of some diatomic molecular hydrides. *Can. J. Phys.* **2021**, *99*, 253. [CrossRef]
25. Okorie, U.S.; Ikot, A.N.; Onyeaju, M.C.; Chukwuocha, E.O. A study of thermodynamic properties of quadratic exponential-type potential in D-dimensions. *Rev. Mex. Física* **2018**, *64*, 608. [CrossRef]
26. Onate, C.A.; Ojonubah, J.O. Eigensolutions of the Schrödinger equation with a class of Yukawa potentials via supersymmetric approach. *J. Theor. Appl. Phys.* **2016**, *10*, 21. [CrossRef]
27. Ciftci, H.; Hall, R.L.; Saad, N. Asymptotic iteration method for eigenvalue problems. *J. Phys. Math. Gen.* **2003**, *36*, 11807. [CrossRef]
28. Bayrak, O.; Boztosun, I. Bound state solutions of the Hulthén potential by using the asymptotic iteration method. *Phys. Scr.* **2007**, *76*, 92. [CrossRef]
29. Edet, C.O.; Ikot, A.N. Effects of Topological Defect on the Energy Spectra and Thermo-magnetic Properties of CO Diatomic Molecule. *J. Low Temp. Phys.* **2021**, *203*, 84. [CrossRef]
30. Nikiforov, A.V.; Uvarov, V.B. *Special Functions of Mathematical Physics*; Birkhauser: Bassel, Switzerland, 1988.
31. Edet, C.O.; Okoi, A.P.O. Any l-state solutions of the Schrödinger equation for q-deformed Hulthen plus generalized inverse quadratic Yukawa potential in arbitrary dimensions. *Rev. Mex. Física* **2019**, *65*, 333. [CrossRef]
32. Tezcan, C.; Sever, R. A general approach for the exact solution of the Schrödinger equation. *Int. J. Theor. Phys.* **2009**, *48*, 337. [CrossRef]
33. Falaye, B.J.; Ikhdair, S.M.; Hamzavi, M. Formula method for bound state problems. *Few-Body Syst.* **2015**, *56*, 63. [CrossRef]
34. Wentzel, G. Eine verallgemeinerung der quantenbedingungen für die zwecke der wellenmechanik. *Z. Phys.* **1926**, *38*, 518. [CrossRef]

35. Ita, B.I.; Louis, H.; Akakuru, O.U.; Nzeata-Ibe, N.A.; Ikeuba, A.I.; Magu, T.O.; Amos, P.I.; Edet, C.O. Approximate Solution to the Schrödinger Equation with Manning-Rosen plus a Class of Yukawa Potential via WKBJ Approximation Method. *Bulg. J. Phys.* **2018**, *45*, 323.
36. Ma, Z.Q.; Xu, B.W. Exact quantization rule and the invariant. *Chin. Acta Phys Sin.* **2006**, *55*, 1571–1579. [CrossRef]
37. Ma, Z.Q.; Xu, B.W. Quantum correction in exact quantization rules. *EPL Europhys. Lett.* **2005**, *69*, 685. [CrossRef]
38. Ebeling, W.; Sokolov, I. *Statistical Thermodynamics and Stochastic Theory of Nonequilibrium Systems*; World Scientific Publishing Company: Singapore, 2005; Volume 8.
39. Pathria, R.K. *Statistical Mechanics*; Butterworth: Washington, DC, USA, 1996.
40. Landsberg, P.T. *Thermodynamics and Statistical Mechanics*; Courier Corporation: North Chelmsford, MA, USA, 2014.
41. Okorie, U.S.; Edet, C.O.; Ikot, A.N.; Rampho, G.J.; Sever, R. Thermodynamic functions for diatomic molecules with modified Kratzer plus screened Coulomb potential. *Indian J. Phys.* **2021**, *95*, 411. [CrossRef]
42. Ikot, A.N.; Lutfuoglu, B.C.; Ngwueke, M.I.; Udoh, M.E.; Zare, S.; Hassanabadi, H. Klein-Gordon equation particles in exponential-type molecule potentials and their thermodynamic properties in D dimensions. *Eur. Phys. J. Plus* **2016**, *131*, 1. [CrossRef]
43. Ikot, A.N.; Okorie, U.S.; Rampho, G.J.; Amadi, P.O.; Edet, C.O.; Akpan, I.O.; Abdullah, H.Y.; Horchani, R. Klein–gordon equation and nonrelativistic thermodynamic properties with improved screened kratzer potential. *J. Low Temp. Phys.* **2021**, *202*, 269. [CrossRef]
44. Hylleraas, E.A. Energy formula and potential distribution of diatomic molecules. *J. Chem. Phys.* **1935**, *3*, 595.
45. Ikot, A.N.; Awoga, O.A.; Ita, B.I. Exact solutions of the Klein–Gordon equation with Hylleraas potential. *Few-Body Syst.* **2012**, *53*539. [CrossRef]
46. Okorie, U.S.; Ikot, A.N.; Edet, C.O.; Rampho, G.J.; Sever, R.; Akpan, I.O. Solutions of the Klein Gordon equation with generalized hyperbolic potential in D-dimensions. *J. Phys. Commun.* **2019**, *3*, 095015. [CrossRef]
47. Edet, C.O.; Ikot, A.N. Analysis of the impact of external fields on the energy spectra and thermo-magnetic properties of N2,I2,CO,NO and HCl diatomic molecules. *Mol. Phys.* **2021**, *119*, e1957170. [CrossRef]
48. Edet, C.O.; Nwbabuzor, P.O.; Ettah, E.B.; Duque, C.A.; Ali, N.; Ikot, A.N.; Mahmoud, S.; Asjad, M. Magneto-transport and thermal properties of the Yukawa potential in cosmic string space-time. *Results Phys.* **2022**, *39*, 105749. [CrossRef]
49. Jia, C.-S.; Wang, C.-W.; Zhang, L.-H.; Peng, X.-L.; Zeng, R.; You, X.-T. Partition function of improved Tietz oscillators. *Chem. Phys. Lett.* **2017**, *676*, 150. [CrossRef]
50. Jia, C.-S.; Zhang, L.-H.; Wang, C.-W. Thermodynamic properties for the lithium dimer. *Chem. Phys. Lett.* **2017**, *667*, 211. [CrossRef]